Check for updates

Site-Specific Antibody Fragment Conjugates for Reversible Staining in Fluorescence Microscopy

Jonathan Schwach,[a] Ksenia Kolobynina,[b] Katharina Brandstetter,[a] Marcus Gerlach,[c] Philipp Ochtrop,[d] Jonas Helma,[c] Christian P. R. Hackenberger,[d, e] Hartmann Harz,[a] M. Cristina Cardoso,[b] Heinrich Leonhardt,[a] and Andreas Stengl*[a]

Antibody conjugates have taken a great leap forward as tools in basic and applied molecular life sciences that was enabled by the development of chemoselective reactions for the site-specific modification of proteins. Antibody-oligonucleotide conjugates combine the antibody's target specificity with the reversible, sequence-encoded binding properties of oligonucleotides like DNAs or peptide nucleic acids (PNAs), allowing sequential imaging of large numbers of targets in a single specimen. In this report, we use the Tub-tag® technology in combination with Cu-catalyzed azide-alkyne cycloaddition for the site-specific conjugation of single DNA and PNA strands to an eGFP-binding nanobody. We show binding of the conjugate to recombinant eGFP and subsequent sequence-specific annealing of fluorescently labelled imager strands. Furthermore, we reversibly stain eGFP-tagged proteins in human cells, thus demonstrating the suitability of our conjugation strategy to generate antibody-oligonucleotides for reversible immunofluorescence imaging.

Introduction

Proteins, especially antibodies, have been widely used as important tools in basic research and more recently as diagnostic and therapeutic agents.[1,2] Site- or residue-specific modification of antibodies with additional moieties ranging from small chemical compounds to large polypeptides has further expanded their field of use. This advancement was enabled by the development of chemoselective or bioorthogonal reactions and incorporation of unnatural amino acids into antibodies.[3] Antibody-oligonucleotide conjugates represent particularly interesting modalities, as they combine two key advantages of their building blocks in a single entity: specific antigen binding of antibodies with sequence-dependent hybridization of oligonucleotides to complementary strands. The former allows specific binding of target proteins in complex contexts such as cells, while the latter can be used for tunable, thus, reversible attachment of additional functionalities such as fluorophores. Unsurprisingly, protein-oligonucleotide conjugates have seen great use in a variety of applications ranging from protein immobilization,[4] bioanalytics[5–7] to material science.[8–10] Moreover, antibody-oligonucleotide conjugates have been employed in fluorescence and super resolution microscopy[11,12] as they resolve the limitations that come with standard fluorophore-conjugated antibodies.

Although fluorophore-conjugated antibodies are one of the most common staining reagents due to their broad spectrum of targets, the virtually irreversible binding of antibodies and the spectral overlap between fluorophores heavily limit the number of individual targets that can be investigated at the same time. To overcome this problem, efforts have been devoted to develop protocols to either elute the antibodies[13,14] or chemically inactivate the fluorophores in between successive imaging rounds. However, these techniques involve harsh washing steps and thereby potentially alter epitope accessibility for the following imaging probes. Thus, elution of the previous probe should ideally be rapid and buffer conditions mild to preserve sample integrity. An elegant way to achieve this goal was developed for super-resolution microscopy called DNA-point accumulation for imaging in nanoscale topography (DNA-PAINT).[15] DNA-PAINT exploits the transient binding of fluorophore-coupled oligonucleotides (imager strands) to their complementary sequence (docking strands) for reversible immobilization. The tunability of the binding strength between

[a] J. Schwach, K. Brandstetter, Dr. H. Harz, Prof. Dr. H. Leonhardt, Dr. A. Stengl
Ludwig-Maximilians-Universität München
Department of Biology II, Human Biology and BioImaging
82152 Planegg-Martinsried (Germany)
E-mail: stengl@bio.lmu.de
stengl.andreas@gmail.com
[b] K. Kolobynina, Prof. Dr. M. C. Cardoso
Technical University of Darmstadt
Department of Biology, Cell Biology and Epigenetics
Schnittspahnstr. 10, 64287 Darmstadt (Germany)
[c] Dr. M. Gerlach, Dr. J. Helma
Tubulis GmbH, BioSysM
Butenandtstrasse 1, 81377 Munich (Germany)
[d] P. Ochtrop, Prof. Dr. C. P. R. Hackenberger
Leibniz-Forschungsinstitut für Molekulare Pharmakologie (FMP)
Department Chemical Biology
Robert-Rössle-Strasse 10, 13125 Berlin (Germany)
[e] Prof. Dr. C. P. R. Hackenberger
Humboldt Universität zu Berlin
Department of Chemistry
Brook-Taylor-Strasse 2, 12489 Berlin (Germany)

Supporting information for this article is available on the WWW under https://doi.org/10.1002/cbic.202000727

This article is part of a joint Special Collection with the Journal of Peptide Science on SPP 1623: Chemoselective reactions for the synthesis and application of functional proteins. Please see our homepage for more articles in the collection.

© 2020 The Authors. ChemBioChem published by Wiley-VCH GmbH. This is an open access article under the terms of the Creative Commons Attribution Non-Commercial License, which permits use, distribution and reproduction in any medium, provided the original work is properly cited and is not used for commercial purposes.

oligonucleotides allows for rapid exchange of fluorophores under mild washing conditions.[16,17]

Techniques to generate oligonucleotide-conjugated antibodies have subsequently received increasing interest. Common protocols involve bifunctional linkers that target exposed residues of amino acids on the protein surface.[18–20] However, conjugation stoichiometry is challenging to control depending on the abundance of the reactive surface residue. Other approaches that allow site-specific conjugation rely on guiding the reaction with a complementary template,[21] the incorporation of unnatural amino acids,[22,23] targeting unique or rare amino acids on native proteins[24] or the use of tag-enzyme pairs.[25–28] We previously established the Tub-tag® conjugation technology for bioorthogonal, chemoenzymatic labelling of proteins[29,30] The Tub-tag® technology makes use of the enzyme tubulin tyrosine ligase (TTL) as a highly flexible tool for protein modification, that accepts a broad range of tyrosine derivatives as substrates enabling various bioorthogonal chemistries. We demonstrated its suitability for functionalization with small molecules[31] as well as protein-protein ligation.[32] In this work, we present the Tub-tag® mediated, efficient and site-specific generation of nanobody-DNA and -PNA conjugates in a 1:1 stoichiometry that can readily be used for reversible staining in confocal fluorescence microscopy.

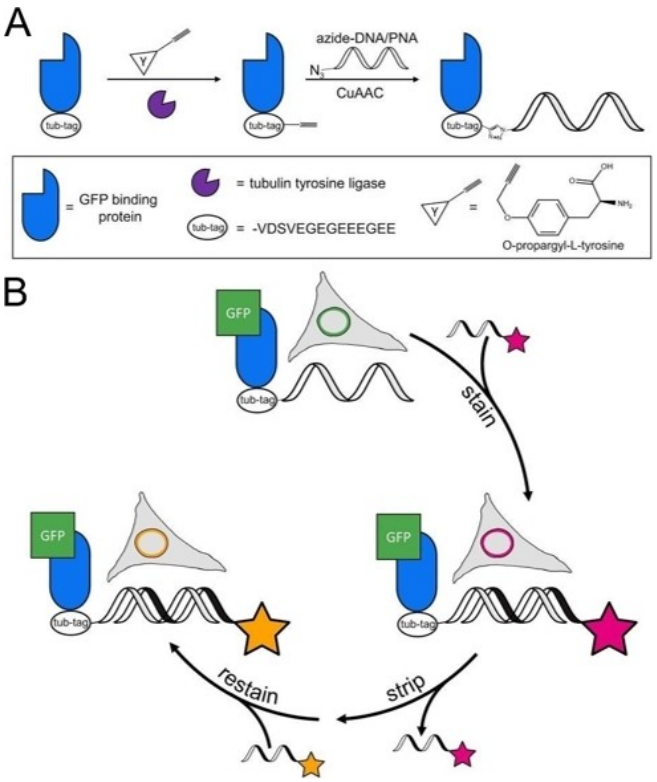

Figure 1. Functionalization strategy for generating nanobody-oligonucleotide conjugates and usage for reversible staining in fluorescence microscopy. A) Schematic representation of the site-specific ligation of single-stranded oligonucleotides to the C terminus of Tub-tagged nanobodies in a two-step process. First, an alkyne handle is introduced by the tubulin-tyrosine ligase (TTL)-catalyzed ligation of *O*-propargyl-L-tyrosine to the Tub-tag. Second, azide-DNA or azide-PNA is conjugated to the alkyne handle by CuAAC. B) Reversible immunofluorescence staining by hybridization of a fluorescent imager strand with the nanobody-oligonucleotide conjugate. Stripping of the imager strand allows for restaining of the sample.

Results and Discussion

Our approach combines enzyme-catalyzed ligation of a reactive chemical handle to an eGFP-binding nanobody (GBP) with Cu^{I}-catalyzed alkyne-azide cycloaddition (CuAAC) to conjugate the oligonucleotide (Figure 1A). As proof-of-principle, we employed these conjugates for reversible staining of eGFP-fusion protein expressing cells in confocal fluorescence microscopy (Figure 1B). In a first step, TTL recognizes the C-terminal Tub-tag® on the protein and site-specifically ligates O-propargyl-L-tyrosine to the C terminus of the antibody. This introduces an alkyne group to the protein that can be used as a chemical handle for following reactions. Second, we used CuAAC for conjugation of an azide-containing DNA or PNA to form a stable bond between antibody and oligonucleotide at a 1:1 stoichiometry. We envisioned that the unique characteristics of PNAs such as higher melting temperature and uncharged backbone would additionally broaden the general applicability of this strategy alternative to DNA conjugation.

We first set out to generate antibody-DNA/-PNA conjugates by using Tub-tag® technology and CuAAC based on previously published optimizations[32] and used eGFP-binding protein as a model antibody fragment. SDS-PAGE and Coomassie staining confirmed efficient conjugation of both azide-DNA (yield: 55.9%) and azide-PNA (yield: 66.1%) to alkyne-modified GBP at 4x molar excess of azide-oligo over nanobody (Figure 2A).

We hypothesized that especially the DNA oligonucleotide would strongly influence the total charge of the conjugated molecule so that unfunctionalized alkynyl GBP can be separated from the conjugate. Therefore, we performed mass spectrometry (Figure S1) and anion-exchange chromatography (AEX) to further validate our observation from the gel electrophoresis. Notably, we observed a strong shift towards higher ionic strength for GBP-DNA conjugate compared to unfunctionalized alkynyl GBP indicating stronger interaction with the stationary phase (Figure 2B). In addition, the GBP-DNA conjugate and free azide-DNA were not separable to baseline, thus suggesting that binding to the stationary phase is mediated by the DNA oligonucleotide to a major degree. Nevertheless, AEX allows for removal of unconjugated alkynyl antibody as demonstrated by SDS-PAGE (Figure 2A) and partial depletion of free DNA in the final product. In contrast, the antibody-PNA conjugates shifted towards lower ionic strengths. In accordance with this observation, free azide-PNA molecules eluted during the column wash because PNA does not have a strong negative charge (Figure 2B).

Taken together, these findings not only confirm that our chemoenzymatic functionalization approach is capable of generating protein-oligonucleotide conjugates with high efficiency, but also that unfunctionalized alkynyl protein is separable from the conjugate product by AEX and free azide-oligonucleotides can be at least partially depleted.

© 2020 The Authors. ChemBioChem published by Wiley-VCH GmbH

14397633, 2021, 7, Downloaded from https://chemistry-europe.onlinelibrary.wiley.com/doi/10.1002/cbic.202000727 by Technische Universitat Darmstadt, Wiley Online Library on [02/01/2024]. See the Terms and Conditions (https://onlinelibrary.wiley.com/terms-and-conditions) on Wiley Online Library for rules of use; OA articles are governed by the applicable Creative Commons License

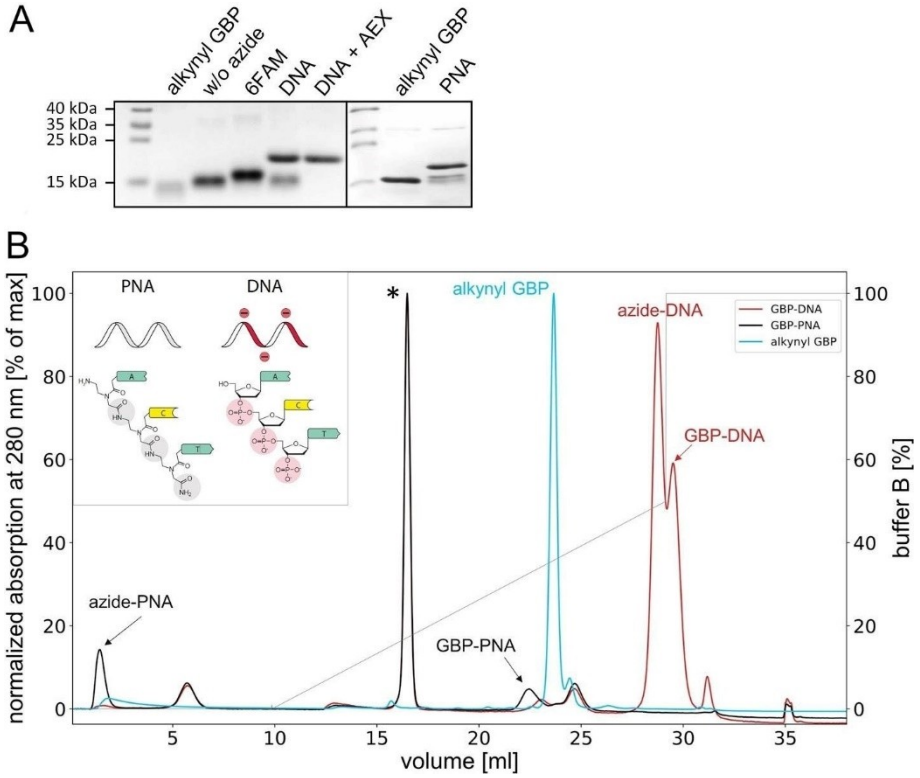

Figure 2. TTL-catalyzed enzymatic incorporation of *O*-propargyl-L-tyrosine and subsequent conjugation of azide-modified 15 bp DNA and PNA strands by CuAAC. A) Coomassie staining of SDS gels of functionalized alkynyl GBP (cropped sections, contrast adjusted, full images can be found in Figure S2). Alkynyl GBP was generated by TTL-catalyzed ligation of *O*-propargyl-L-tyrosine (298 μM GBP-TT, 29.8 μM TTL and 10 mM *O*-propargyl-L-tyrosine for 3 h at 30 °C). Conjugation with azide-DNA was performed by using 40 μM akynyl GBP and 160 μM azide-DNA; conjugation with azide-PNA was performed by using 60 μM alkynyl GBP and 120 μM azide-PNA (0.25 mM $CuSO_4$, 1.25 mM THPTA, 5 mM aminoguanidine and 5 mM sodium ascorbate). B) Analytical anion-exchange chromatography of the raw conjugation products of (A). Absorption (280 nm) is normalized to the strongest signal. The peak marked with an asterisk represents EDTA (Figure S3).

To determine whether the antibody-oligonucleotide can bind both target and the complementary imager strand, we performed an *in vitro* binding assay on immobilized purified protein using either eGFP (target) or BSA (negative control). We detected strong signals for both DNA and PNA conjugate when the sample was hybridized with the complementary imager DNA-strand. Using either BSA as target protein or a non-complementary imager strand lead only to a minor increase of fluorescence (Figure 3 top). This result confirmed that the functionality of both the antibody and the DNA docking strand was preserved by our conjugation strategy, as our conjugate was able to bind both eGFP and the complementary imager strand. Based on these findings, we were prompted to test our conjugate on fixed cells, which provide a much more complex environment that could potentially lead to a higher degree of unspecific staining. Therefore, we used transiently transfected HEK293F cells expressing eGFP-actin fusion protein, and repeated the staining similar to the previous experiment (Figure 3, bottom). We observed the strongest signal in eGFP-actin-transfected cells when staining with the complementary imager strand. Untransfected cells that do not express eGFP did not show elevated levels of fluorescence in the imager strand channel. Staining with noncomplementary imager strand resulted in a minor increase of background fluorescence in both transfected and untransfected cells, suggesting that this effect is inherent to unspecific binding of the DNA or fluorophore itself to cellular components but not due to interaction with the docking strand. Antibody-PNA conjugate yielded higher fluorescence intensity, potentially indicating stronger binding of the DNA imager strand to PNA than to DNA as reported previously.[33]

These promising results encouraged us to test whether the conjugate can be used for reversible immunostaining in confocal fluorescence microscopy. To this end, we stained fixed HEK293F and HeLa cells expressing either eGFP-LaminB1 or eGFP-PCNA fusion proteins, respectively, with DNA-conjugated nanobody. To verify that the imager strand can be detached from the docking strand, we stripped the samples with formamide containing buffer and performed restaining using an imager strand with the same sequence but different fluorophore as visualized in Figure 1B. For both target proteins, we observed distinct nuclear staining with strong colocalization of imager strand and eGFP-LaminB1 or eGFP-PCNA, respectively (Figure 4). After stripping off the first imager strand, we detected practically no remaining fluorescence although we used a highly sensitive detector, thus suggesting that the imager strand was efficiently detached from the DNA-docking strand. Restaining with a second imager strand led again to

© 2020 The Authors. ChemBioChem published by Wiley-VCH GmbH

14397633, 2021, 7, Downloaded from https://chemistry-europe.onlinelibrary.wiley.com/doi/10.1002/cbic.202000727 by Technische Universitat Darmstadt, Wiley Online Library on [02/01/2024]. See the Terms and Conditions (https://onlinelibrary.wiley.com/terms-and-conditions) on Wiley Online Library for rules of use; OA articles are governed by the applicable Creative Commons License

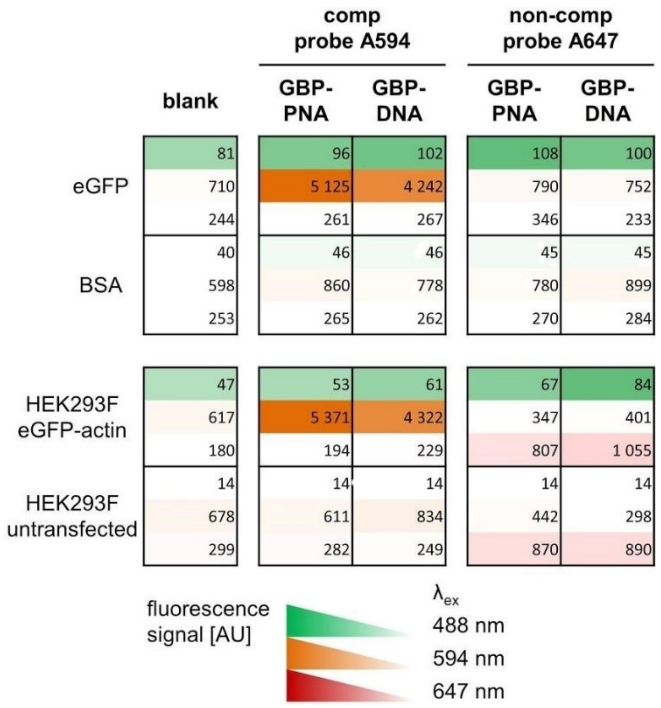

Figure 3. Nanobody-oligonucleotide conjugates exhibit bind to their target protein and allow sequence-specific annealing of fluorescently labelled imager strands. Top: Binding of nanobody-oligonucleotide conjugates to purified eGFP and annealing of a either complementary fluorescent imager strand (comp probe A594) or noncomplementary fluorescent imager strand (non-comp probe A647). Bottom: Binding of nanobody-oligonucleotide conjugates to eGFP-actin expressing cells. Imager strands were used as in the top panels. Fluorescence signal intensity per well is represented by the respective color coding.

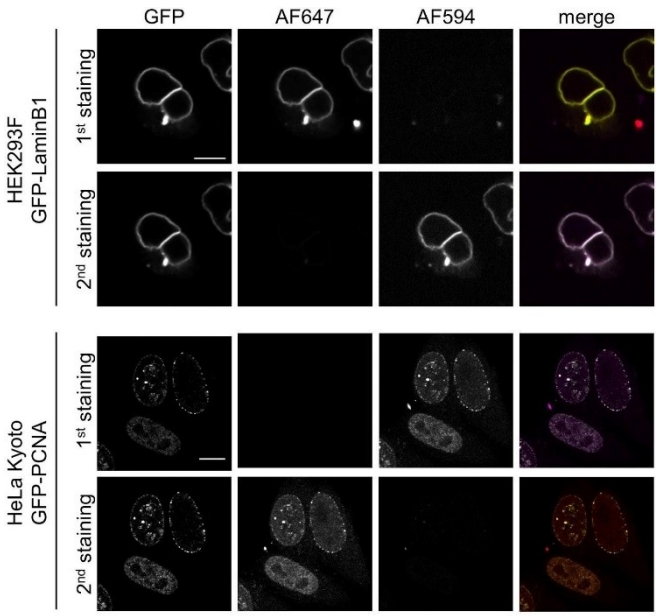

Figure 4. Nanobody-oligonucleotide conjugates are suitable for reversible staining of cells in fluorescence microscopy. Top: Staining of HEK293F cells expressing eGFP-LaminB1. eGFP-LaminB1 is stained by binding of the nanobody-DNA conjugate and subsequent annealing of a complementary imager strand leading to colocalized signal of imager strand and eGFP. Disruption of the interaction of imager and docking strand leads to almost complete removal of fluorescence, allowing for restaining with a complementary imager strand in a different channel. Bottom: Staining of HeLa Kyoto cells expressing eGFP-PCNA. Staining was performed identically to the top panel. Scale bars: 10 μm.

colocalization of eGFP and imager strand fluorescence (Figure 4). Thus, this result demonstrates that the nanobody-DNA conjugate remains intact during the washing and that the staining is reversible. In contrast, nanobody-PNA conjugates showed residual fluorescence after washing in cell staining (Figure S4) as well as *in vitro* binding assays (Figure S5). This observation is potentially due to stronger hybridization of PNA/DNA duplexes and might be resolved by optimization of washing conditions or altering the sequence to lower hybridization temperatures. For nanobody-DNA and -PNA conjugates, we observed minor background staining of the nucleus in all cells even without expression of eGFP (Figure S6); this supports the assumption that the background is likely caused by nonspecific interaction of the DNA-imager strand with genomic DNA.

In summary, we have shown herein a novel conjugation technique for generation of nanobody-DNA and -PNA conjugates. Our approach allows the site-specific conjugation in 1:1 stoichiometry with high efficiency as shown by SDS-PAGE and anion-exchange chromatography. In addition, binding assays on immobilized protein show a strong and specific staining towards the epitope of the antibody. Moreover, we demonstrate quick and efficient reversibility of the staining by using confocal fluorescence microscopy, which is a key requirement for multiplexing via fluorophore exchange. Thus, our technology provides a new tool for chemo-enzymatic generation of protein-oligonucleotide conjugates. The defined 1:1 stoichiometry of our conjugation strategy provides a valuable advantage over currently state-of-the-art functionalization of surface exposed amino acids, where neither the stoichiometry nor the functionalization site is defined.

Acknowledgements

We thank Hans C. Mescheder for countless scientific conversations and critical suggestions contributing to the advancement of this project. Furthermore, we thank Dominik Schumacher for scientific input regarding the Tub-tag® technology. This work was supported by grants from the Deutsche Forschungsgemeinschaft (DFG, German Research Foundation) within the SPP1623 to C.P.R.H. (HA 4468/9-1, 9-2 and 10-2), H.L. (LE 721/13-1, 13-2) and M.C.C. (CA 198/8-1, 8-2), GRK1657/TP1B to M.C.C., GRK1721 to H.L. and the Leibniz Association with the Leibniz Wettbewerb (T18/2017) to C.P.R.H and H.L.. Open access funding enabled and organized by Projekt DEAL.

© 2020 The Authors. ChemBioChem published by Wiley-VCH GmbH

14397633, 2021, 7, Downloaded from https://chemistry-europe.onlinelibrary.wiley.com/doi/10.1002/cbic.202000727 by Technische Universitat Darmstadt, Wiley Online Library on [02/01/2024]. See the Terms and Conditions (https://onlinelibrary.wiley.com/terms-and-conditions) on Wiley Online Library for rules of use; OA articles are governed by the applicable Creative Commons License

Keywords: antibody conjugates · immunofluorescence staining · nanobodies · peptide nucleic acids · super-resolution microscopy · Tub-tag labelling

[1] D. Schumacher, C. P. Hackenberger, *Curr. Opin. Chem. Biol.* **2014**, *22*, 62–69.
[2] J. Helma, M. C. Cardoso, S. Muyldermans, H. Leonhardt, *J. Cell Biol.* **2015**, *209*, 633–644.
[3] K. Lang, J. W. Chin, *ACS Chem. Biol.* **2014**, *9*, 16–20.
[4] Z. Zhao, J. Fu, S. Dhakal, A. Johnson-Buck, M. Liu, T. Zhang, N. W. Woodbury, Y. Liu, N. G. Walter, H. Yan, *Nat. Commun.* **2016**, *7*, 10619.
[5] Y. Xiang, Y. Lu, *Nat. Chem.* **2011**, *3*, 697–703.
[6] J. A. G. L. van Buggenum, J. P. Gerlach, S. Eising, L. Schoonen, R. A. P. M. van Eijl, S. E. J. Tanis, M. Hogeweg, N. C. Hubner, J. C. van Hest, K. M. Bonger, K. W. Mulder, *Sci. Rep.* **2016**, *6*, 22675.
[7] J. Wiener, D. Kokotek, S. Rosowski, H. Lickert, M. Meier, *Sci. Rep.* **2020**, *10*, 1457–1457.
[8] C. Hou, S. Guan, R. Wang, W. Zhang, F. Meng, L. Zhao, J. Xu, J. Liu, *J. Phys. Chem. Lett.* **2017**, *8*, 3970–3979.
[9] J. R. McMillan, C. A. Mirkin, *J. Am. Chem. Soc.* **2018**, *140*, 6776–6779.
[10] L. Gogolin, H. Schroeder, A. Itzen, R. S. Goody, C. M. Niemeyer, C. F. W. Becker, *ChemBioChem* **2013**, *14*, 92–99.
[11] S. S. Agasti, Y. Wang, F. Schueder, A. Sukumar, R. Jungmann, P. Yin, *Chem. Sci.* **2017**, *8*, 3080–3091.
[12] F. Schueder, M. T. Strauss, D. Hoerl, J. Schnitzbauer, T. Schlichthaerle, S. Strauss, P. Yin, H. Harz, H. Leonhardt, R. Jungmann, *Angew. Chem. Int. Ed.* **2017**, *56*, 4052–4055; *Angew. Chem.* **2017**, *129*, 4111–4114.
[13] C. Wählby, F. Erlandsson, E. Bengtsson, A. Zetterberg, *Cytometry* **2002**, *47*, 32–41.
[14] K. D. Micheva, S. J. Smith, *Neuron* **2007**, *55*, 25–36.
[15] R. Jungmann, C. Steinhauer, M. Scheible, A. Kuzyk, P. Tinnefeld, F. C. Simmel, *Nano Lett.* **2010**, *10*, 4756–4761.
[16] R. Jungmann, M. S. Avendaño, J. B. Woehrstein, M. Dai, W. M. Shih, P. Yin, *Nat. Methods* **2014**, *11*, 313.
[17] Y. Wang, J. B. Woehrstein, N. Donoghue, M. Dai, M. S. Avendaño, R. C. J. Schackmann, J. J. Zoeller, S. S. H. Wang, P. W. Tillberg, D. Park, S. W. Lapan, E. S. Boyden, J. S. Brugge, P. S. Kaeser, G. M. Church, S. S. Agasti, R. Jungmann, P. Yin, *Nano Lett.* **2017**, *17*, 6131–6139.
[18] C. M. Niemeyer, T. Sano, C. L. Smith, C. R. Cantor, *Nucleic Acids Res.* **1994**, *22*, 5530–5539.
[19] H. Gong, I. Holcomb, A. Ooi, X. Wang, D. Majonis, M. A. Unger, R. Ramakrishnan, *Bioconjugate Chem.* **2016**, *27*, 217–225.
[20] A. V. Maerle, M. A. Simonova, V. D. Pivovarov, D. V. Voronina, P. E. Drobyazina, D. Y. Trofimov, L. P. Alekseev, S. K. Zavriev, D. Y. Ryazantsev, *PLoS One* **2019**, *14*, e0209860.
[21] C. B. Rosen, A. L. B. Kodal, J. S. Nielsen, D. H. Schaffert, C. Scavenius, A. H. Okholm, N. V. Voigt, J. J. Enghild, J. Kjems, T. Tørring, K. V. Gothelf, *Nat. Chem.* **2014**, *6*, 804–809.
[22] K. Lang, J. W. Chin, *Chem. Rev.* **2014**, *114*, 4764–4806.
[23] D. Katrekar, A. M. Moreno, G. Chen, A. Worlikar, P. Mali, *Sci. Rep.* **2018**, *8*, 3589.
[24] M.-A. Kasper, M. Glanz, A. Stengl, M. Penkert, S. Klenk, T. Sauer, D. Schumacher, J. Helma, E. Krause, M. C. Cardoso, H. Leonhardt, C. Hackenberger, *Angew. Chem. Int. Ed.* **2019**, *54*, 11625–11630.
[25] M. W.-L. Popp, J. M. Antos, H. L. Ploegh, *Curr. Protocols Protein Sci.* **2009**, *56*, 15.13.11-15.13.19.
[26] D. Rabuka, J. S. Rush, G. W. deHart, P. Wu, C. R. Bertozzi, *Nat. Protoc.* **2012**, *7*, 1052–1067.
[27] V. Siegmund, S. Schmelz, S. Dickgiesser, J. Beck, A. Ebenig, H. Fittler, H. Frauendorf, B. Piater, U. A. K. Betz, O. Avrutina, A. Scrima, H.-L. Fuchsbauer, H. Kolmar, *Angew. Chem. Int. Ed.* **2015**, *54*, 13420–13424; *Angew. Chem.* **2015**, *127*, 13618–13623.
[28] M. Rashidian, J. K. Dozier, M. D. Distefano, *Bioconjugate Chem.* **2013**, *24*, 1277–1294.
[29] D. Schumacher, J. Helma, F. A. Mann, G. Pichler, F. Natale, E. Krause, M. C. Cardoso, C. P. Hackenberger, H. Leonhardt, *Angew. Chem. Int. Ed.* **2015**, *54*, 13787–13791; *Angew. Chem.* **2015**, *127*, 13992–13996.
[30] D. Schumacher, O. Lemke, J. Helma, L. Gerszonowicz, V. Waller, T. Stoschek, P. M. Durkin, N. Budisa, H. Leonhardt, B. G. Keller, C. P. R. Hackenberger, *Chem. Sci.* **2017**, *8*, 3471–3478.
[31] M. Effenberger, A. Stengl, K. Schober, M. Gerget, M. Kampick, T. R. Müller, D. Schumacher, J. Helma, H. Leonhardt, D. H. Busch, *J. Immunol.* **2019**, ji1801435.
[32] A. Stengl, M. Gerlach, M.-A. Kasper, C. P. R. Hackenberger, H. Leonhardt, D. Schumacher, J. Helma, *Org. Biomol. Chem.* **2019**, *17*, 4964–4969.
[33] M. C. Chakrabarti, F. P. Schwarz, *Nucleic Acids Res.* **1999**, *27*, 4801–4806.

Manuscript received: October 21, 2020
Revised manuscript received: November 17, 2020
Accepted manuscript online: November 18, 2020
Version of record online: December 17, 2020

© 2020 The Authors. ChemBioChem published by Wiley-VCH GmbH

14397633, 2021, 7, Downloaded from https://chemistry-europe.onlinelibrary.wiley.com/doi/10.1002/cbic.202000727 by Technische Universitat Darmstadt, Wiley Online Library on [02/01/2024]. See the Terms and Conditions (https://onlinelibrary.wiley.com/terms-and-conditions) on Wiley Online Library for rules of use; OA articles are governed by the applicable Creative Commons License